

## Theory of Electron Mediated Mn-Mn Interactions in Quantum Dots

Fanyao Qu and Pawel Hawrylak

*Institute for Microstructural Sciences, National Research Council of Canada, Ottawa, K1A 0R6, Canada*

*Department of Physics, University of Ottawa, Ottawa, K1N 6N5, Canada*

(Received 28 December 2005; published 20 April 2006)

We present a theory of interaction of magnetic Mn ions depending strongly on the number ( $Ne$ ) of electrons in a quantum dot. For closed electronic shells, we derive the RKKY interaction and its dependence on magnetic ion positions, quantum dot energy quantization  $\omega_0$ , and the number of filled shells  $Ns$ . For partially filled shells, the many-electron magnetopolaron effect leads to effective carrier mediated ferromagnetic Mn-Mn interactions. The dependence of the magnetopolaron energy on magnetic ion positions, quantum dot energy quantization  $\omega_0$ , and the number of electrons  $Ne$  is predicted.

DOI: [10.1103/PhysRevLett.96.157201](https://doi.org/10.1103/PhysRevLett.96.157201)

PACS numbers: 75.75.+a, 73.21.La, 75.50.Pp, 78.67.Hc

The problem of the interaction of magnetic ions controlled by free carriers is of interest in a number of areas of condensed matter physics, from nanospintronics [1,2], creating and controlling magnetic properties of bulk and low-dimensional semiconductors [3–16], to the competition of Kondo and RKKY physics in heavy fermions and mixed valence compounds [17,18]. Attempts to create hybrid systems consisting of few magnetic ions in a controlled electronic environment include few magnetic ions probed optically in CdTe quantum dots [12,13], on a surface of a solid probed by a spin-flip STM [2], in bulk GaAs [7] by STM, and in both Mn-doped nanocrystals [8–10] as well as quantum dot tunneling devices embedded in a magnetic barrier [11]. Theoretically, interaction of carriers with magnetic impurities in quantum wells [5,6], nanocrystals [8,9], and quantum dots [4,13–16] has been investigated, including both mean field theory of noninteracting electrons interacting with a large number of Mn ions [14] as well as few-particle effects coupled with a single Mn ion [15,16]. In this Letter, we present a theory of carrier mediated interaction of magnetic Mn ions placed in a controlled, strongly interacting, electronic environment provided by a quantum dot (QD) filled with  $Ne$  electrons, an artificial atom. The quantum dot allows for engineering of total electron spin and the electron-Mn interaction by tuning the electron number  $Ne$  with gates. Recent advances in controlled positioning of impurities in solids [2,7] allow us to anticipate future control over the position of Mn ions. We focus here on self-assembled quantum dots with well-defined electronic shells [19] where the number of electrons is controlled by external gates [20]. The electronic ground states correspond to spin singlet closed shell configurations for  $Ne = 2, 6, 12, \dots$ , while for partial shell filling total spin is maximized according to Hund's rules [19,20]. We find that the carrier mediated Mn-Mn interaction can be grouped into two distinct classes controlled by the number of electrons in the dot. For electron numbers corresponding to closed shells, we find oscillatory RKKY interaction, while for electron numbers corresponding to partially filled shells, electron-electron interaction leads to

electron spin polarization, and the Mn-Mn interaction is found to be mediated by many-electron magnetopolaron effects.

We consider a quasi-two-dimensional quantum dot with parabolic confinement, a model suitable for self-assembled quantum dots [19], containing  $Ne$  interacting electrons and a pair of magnetic Mn ions at positions  $R_1$  and  $R_2$ . The pair of magnetic ions is treated here as a starting point for a many-Mn system. The single-particle states and energies of an electron in a parabolic QD correspond to two coupled harmonic oscillators with quantum numbers  $m$  and  $n$ ,  $\varphi_{mn}(x, y) = \varphi_m(x)\varphi_n(y)$ , where  $x$  and  $y$  are electron coordinates in the plane of the quantum dot, with  $z$  being the growth direction. The lowest three one-dimensional harmonic oscillator states are  $\varphi_0(\hat{x}) = e^{-\hat{x}^2/4}/(2\pi\ell_0^2)^{1/4}$ ,  $\varphi_1(\hat{x}) = \hat{x}e^{-\hat{x}^2/4}/(2\pi\ell_0^2)^{1/4}$ , and  $\varphi_2(\hat{x}) = (\hat{x}^2 - 1)e^{-\hat{x}^2/4}/(8\pi\ell_0^2)^{1/4}$ , with  $\hat{x} = x/\ell_0$  and  $\ell_0 = 1/\sqrt{\omega_0}$ . Here  $\omega_0$  is shell spacing, and length and energy are measured in effective Bohr radius  $a_B$  and effective Rydberg  $Ry$ . The single-particle energies  $E_{nm} = (n + m + 1)\omega_0$  form degenerate electronic shells with degeneracy  $g_s = s + 1$  ( $s = n + m$ ) and shell spacing  $\omega_0$ . The electron-Mn  $sp-d$  exchange interaction is modeled here by a contact ferromagnetic interaction [3]  $\hat{H}_{e-Mn} = -J_c^{2D} \vec{M} \cdot \vec{S} \delta(\vec{r} - \vec{R})$ , where  $\vec{S}(\vec{M})$  is electron (Mn) spin,  $\vec{r}(\vec{R})$  is electron (Mn) position, and  $J_c^{2D} = J_c 2/d$  is interaction strength, with  $d$  the thickness of the quantum dot. The antiferromagnetic Mn-Mn interaction  $\hat{H}_{Mn-Mn} = J_{12} \vec{M}_1 \cdot \vec{M}_2$  is proportional to the exchange coupling parameter  $J_{12} = J_{12}^{(0)} \exp\{-\lambda[(R_{12}/a_0) - 1]\}$ , which strongly depends upon a separation  $R_{12} = R_1 - R_2$  between two Mn ions. Here  $a_0$  is a lattice constant and  $J_{12}^{(0)}$  is a nearest-neighbor interaction. The strength  $J_{12}$  of exchange coupling between the Mn ion and its next-nearest neighbor is reflected in the value of  $\lambda$ . We choose  $\lambda = 5.1$ , corresponding to  $J_{12}$  for the interaction between the next neighbor Mn ions, about 12% of  $J_{12}^{(0)}$  which is consistent with experimental measurement [21].

Following Ref. [16], we write the many-electron many-Mn Hamiltonian in second quantization form. Denoting annihilation (creation)  $c_{i,\sigma}$  ( $c_{i,\sigma}^+$ ) operators for electrons in single-particle states  $\{n, m\} = \{i\}$  and using Mn spin rising and lowering operators  $M^+$ ,  $M^-$ , the Hamiltonian can be written as:

$$\begin{aligned} \hat{H} = & g_{\text{Mn}}\mu_B B M_1^z + g_{\text{Mn}}\mu_B B M_2^z + J_{12}\vec{M}_1 \cdot \vec{M}_2 \\ & - \sum_{i,j,l} \frac{J_{ij}(R_l)}{2} [(c_{i,\uparrow}^+ c_{j,\uparrow} - c_{i,\downarrow}^+ c_{j,\downarrow}) M_l^z + c_{i,\downarrow}^+ c_{j,\uparrow} M_l^+ \\ & + c_{i,\uparrow}^+ c_{j,\downarrow} M_l^-] + \sum_{i\sigma} E_{i,\sigma} c_{i,\sigma}^+ c_{i,\sigma} \\ & + \frac{1}{2} \sum_{ijkl} \langle i, j | V_{ee} | k, l \rangle c_{i,\sigma}^+ c_{j,\sigma'}^+ c_{k,\sigma'} c_{l,\sigma}. \end{aligned} \quad (1)$$

The first line in Eq. (1) is the Hamiltonian of the Mn subsystem, including Mn-Mn interactions. The fourth term describes the interaction of Mn ions with electrons. It consists of three terms. The first term measures difference in spin up and down population and acts as electron Zeeman energy in the field of a magnetic ion as well as a source of electron spin conserving scattering. The second and third terms involve scattering accompanied by the flipping of electron spin compensated by the flipping of Mn spin. The  $e$ -Mn interaction strength is proportional to the electron-Mn exchange matrix elements  $J_{ij}(R_l) = J_C^{2D} \varphi_i^*(R_l) \varphi_j(R_l)$  determined by the wave function of the two states “ $i$ ” and “ $j$ ” at the position  $R_l$  of the  $l$ th Mn ion. Hence, the effect of Mn is to introduce spin-related disorder. The last two terms in Eq. (1) describe the electron Hamiltonian, with  $E_{i,\sigma}$  the energy of an electron on the single-particle orbital  $|i\rangle$  with spin  $\sigma_i$  and  $\langle i, j | V_{ee} | k, l \rangle$  two-body Coulomb matrix elements. Here  $g_{\text{Mn}}$  ( $g_e$ ) is the Mn (electron)  $g$  factor,  $\mu_B$  is the Bohr magneton, and  $B$  is the magnetic field along the  $z$  axis. In what follows, we adopt  $J_c = 15 \text{ eV } \text{\AA}^3$ ,  $J_{12}^{(0)} = 0.5 \text{ meV}$ ,  $d = 2 \text{ nm}$ ,  $\varepsilon = 10.6$ ,  $m^* = 0.106$ , Bohr radius  $a_B = 52.9 \text{ \AA}$ ,  $\text{Ry} = 12.8 \text{ meV}$ ,  $g_e = -1.67$ ,  $g_{\text{Mn}} = 2.02$ ,  $a_0 = 0.54 \text{ nm}$  with typical  $\omega_0 = 4\text{Ry}$  and effective width  $l_0 = 26.45 \text{ \AA}$ , applicable to II-VI (Cd, Mn)Te semiconductor QDs.

To calculate the electronic properties of the interacting electron-Mn system, we expand the wave function in the following basis of configurations  $|k\rangle$ :  $|k\rangle = |i_1, i_2, \dots, i_{N\uparrow}\rangle \times |j_1, j_2, \dots, j_{N\downarrow}\rangle |M_1^z M_2^z\rangle$ , where  $|i_1, i_2, \dots, i_{N\uparrow}\rangle = c_{i_1,\uparrow}^+ c_{i_2,\uparrow}^+ \dots c_{i_{N\uparrow},\uparrow}^+ |0\rangle$ ,  $|0\rangle$  is the vacuum, and  $N\uparrow$  ( $N\downarrow$ ) is the number of spin up (down) electrons,  $N\uparrow + N\downarrow = N_e$ . The basis states are grouped into spin up and spin down electron states for each configuration of Mn ions  $|M_1^z M_2^z\rangle$ , with  $M_l^z = \pm 5/2, \pm 3/2, \pm 1/2$ . The number of possible electronic and magnetic configurations  $N_C$  is determined by the number of single-particle orbitals  $N_S$ , the number of electrons, the size  $M$  of the magnetic ion spin, and their number  $N_{\text{Mn}}$ , given by  $N_C = (2M + 1)^{N_{\text{Mn}}} \sum_{N_l=0}^N \binom{N_S}{N_l} \binom{N_S}{N_l}$ . Using the basis states, we build the Hamiltonian matrix which

upon diagonalization gives the eigenenergies and eigenstates of the interacting Mn and electron complex. The purpose of this work is to determine the effective Mn-Mn interaction in the presence of electrons. The strength of carrier induced Mn-Mn interaction can be measured in terms of energy shift  $\Delta = E_c - E_e$ , defined by the difference between the ground state energy  $E_c$  of a quantum dot containing both  $N_{\text{Mn}}$  Mn ions and  $N_e$  electrons, and energy  $E_e$  of a quantum dot with only electrons. Note that the presence of Mn ions removes angular momentum and spin conservation and significantly increases computational effort.

Let us first discuss Mn-Mn interaction for closed electronic shells, the quantum dot analog of RKKY interaction in metals [17]. The simplest example is for two electrons in an  $s$  shell. Because of the singlet electronic ground state, there is no direct coupling of electron spin with Mn spins. To gain insight, we evaluate the effect of the electron-Mn interaction on the shift in ground state energy  $\Delta$  in second order perturbation theory as  $\Delta = \sum_k \langle G | H_{e-\text{Mn}} | k \rangle \times \langle k | H_{e-\text{Mn}} | G \rangle / (E_G - E_k)$ , where  $|G\rangle$  is the noninteracting ground state and  $|k\rangle$  is the noninteracting excited configuration. After some algebra, the effect of carriers can be expressed in terms of effective Mn-Mn interaction Hamiltonian  $\Delta = J(\vec{R}_1, \vec{R}_2) \vec{M}_1 \cdot \vec{M}_2$ , with effective RKKY-like interaction strength  $J(\vec{R}_1, \vec{R}_2)$ . Using the analytical form of the single-particle wave functions, an analytical form can be derived for the interaction strength as a function of Mn positions:

$$\begin{aligned} J(\vec{R}_1, \vec{R}_2) = & - \left( \frac{J_c^{2D}}{\pi l_0^2} \right)^2 \left( \frac{1}{4\omega_0} \right) \left\{ \alpha \vec{R}_1 \cdot \vec{R}_2 \right. \\ & \left. + \beta \frac{(\vec{R}_1 \cdot \vec{R}_2)^2 - (\vec{R}_1^2 + \vec{R}_2^2) + 2}{4} \right\} e^{-(\vec{R}_1^2 + \vec{R}_2^2)/2}, \end{aligned} \quad (2)$$

where Mn positions are measured in quantum dot length  $\ell_0$ , and  $\alpha$  and  $\beta$  are parameters controlled by the number of shells and electron-electron interactions. For a quantum dot with only  $s$  and  $p$  shells,  $\beta = 0$ , while for a quantum dot with  $s$ ,  $p$ , and  $d$  shells, we find  $\alpha = 1.0$  and  $\beta = 1.0$ . Including  $e-e$  interactions renormalizes the many-particle energy spectrum and gives  $\alpha = 3.59$  and  $\beta = 2.57$ . The characteristic energy scale is proportional to the square of the ratio of the 2D exchange constant (in units of energy  $\times$  area) divided by the characteristic area of the quantum dot and divided by the shell spacing of the quantum dot, denoted as  $J_0 = (J_c^{2D} / \pi l_0^2)^2 (1/4\omega_0)$ . The smaller the quantum dot, the stronger the RKKY interaction. The interaction decays exponentially with both Mn ions moving away from the center of the dot but can be attractive or negative, depending on Mn positions inside the quantum dot. If we place one Mn ion in the center of the dot,  $R_1 = 0$ , the RKKY interaction should vary as  $J(0, \vec{R}_2) = -(J_c^{2D} / \pi l_0^2)^2 (1/4\omega_0) [\beta(2 - \vec{R}_2^2)/4] e^{-\vec{R}_2^2/2}$  with the position of a second Mn ion. This isotropic interaction is

ferromagnetic for  $R_2 < 2^{1/2}$  and antiferromagnetic for  $R_2 > 2^{1/2}$ . The results of exact diagonalization of the full Hamiltonian, Eq. (1), for  $Ne = 2$  and two Mn ions, in the absence of magnetic field, are shown in Fig. 1. Figure 1 shows the effective RKKY-like interaction strength  $J(\vec{R}_1, \vec{R}_2)$  as a function of the position of the second Mn ion with the first ion in the center. The interaction strength  $J(\vec{R}_1, \vec{R}_2)$  is very well described by the analytical expression discussed above, with the ferromagnetic to antiferromagnetic transition at  $R_2 \sim 2^{1/2}$ . The inset shows a map of  $J(\vec{R}_1, \vec{R}_2)$  as a function of  $R_2$  showing isotropic dependence and the regions with ferromagnetic and antiferromagnetic RKKY coupling. Similar complex maps can be obtained for different Mn ion positions. In Fig. 2(a), we show the map of interaction strength  $J(\vec{R}_1, \vec{R}_2)$  as a function of  $R_2$  for  $R_1 = (1, 0)$ . We see that the RKKY interaction is positive (ferromagnetic) when the two ions are close together but becomes negative (antiferromagnetic) when the second Mn ion is moved to the opposite side of the quantum dot, in agreement with the analytical expression in Eq. (2). To engineer Mn-Mn interactions, we can also change the number of carriers. Figure 2(b) shows the plot of the interaction strength  $J(\vec{R}_1, \vec{R}_2)$  as a function of  $R_2$  but for a quantum dot with two filled shells ( $Ne = 6$ ). We see that,

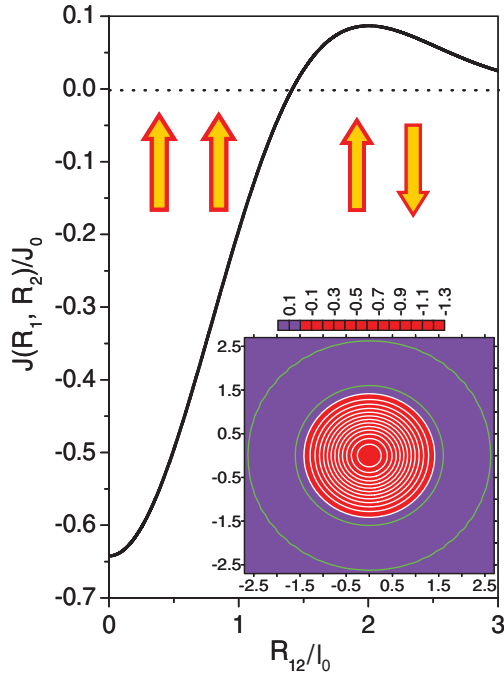


FIG. 1 (color). RKKY interaction strength  $J(R_1, R_2)$  as a function of Mn-Mn separation for a quantum dot containing two electrons and two Mn ions. One Mn ion is located at the center of the quantum dot  $R_1 = 0$  and the second one on the  $x$  axis. The dotted line indicates the change of the sign of  $J(R_1, R_2)$ , and arrows schematically indicate the preferred orientation of Mn spins. The inset shows the spatial map of RKKY interaction strength  $J(0, R_2)$ , with red indicating negative, i.e., ferromagnetic coupling.

in addition to the behavior shown in Fig. 2(a), there are new regions of ferromagnetic and antiferromagnetic coupling constant. This demonstrates the possibility of engineering carrier mediated RKKY interaction in quantum dots with Mn position, shell spacing, and the number of filled shells.

Let us now turn to partially filled shells. For partially filled shells, electron spins couple directly to Mn spins, resulting in a strongly coupled system, the magnetopolaron. The existence of magnetopolarons in quantum dots has been predicted already in Ref. [4]. The polaron effect can be illustrated by considering a single electron in the  $s$  shell. Retaining only  $s$  shell electronic states, assuming  $R_1 = -R_2$ , i.e.,  $J_{ss}(R_1) = J_{ss}(R_2)$ , allows us to introduce total Mn spin  $\vec{M} = \vec{M}_1 + \vec{M}_2$ . Neglecting electron energy and setting magnetic field  $B = 0$ , we obtain a simplified one electron two Mn ions Hamiltonian:

$$\hat{H} = \frac{J_{12}}{2} (\vec{M}^2 - \vec{M}_1^2 - \vec{M}_2^2) - \frac{J_{ss}}{2} [(c_{s,\uparrow}^+ c_{s,\uparrow} - c_{s,\downarrow}^+ c_{s,\downarrow}) M^z + c_{s,\downarrow}^+ c_{s,\uparrow} M^+ + c_{s,\uparrow}^+ c_{s,\downarrow} M^-]. \quad (3)$$

The first term corresponds to short ranged Mn-Mn antiferromagnetic interaction classified by total Mn spin  $0 \leq M \leq M_1 + M_2$ . The second term describes ferromagnetic electron-Mn interaction. Noting that  $M$  is a good quantum number, expanding eigenstates in the basis  $c_{s,\uparrow}^+ |0\rangle |M, M^z\rangle$  and  $c_{s,\downarrow}^+ |0\rangle |M, M^z\rangle$ , allows us to exactly diagonalize the

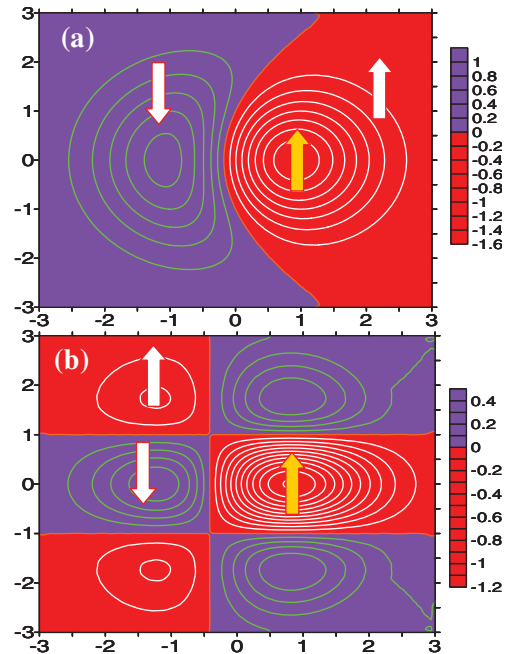


FIG. 2 (color). Maps of RKKY interaction strength  $J(R_1, R_2)$  as a function of the position of the second magnetic impurity  $R_2$  for  $R_1 = 1$  in a quantum dot containing (a) two and (b) six interacting electrons. The red color indicates negative, i.e., ferromagnetic coupling, while blue indicates positive, i.e., antiferromagnetic coupling. The first Mn is indicated by a yellow arrow. The white arrows show different orientations of the second Mn ion depending on its position.

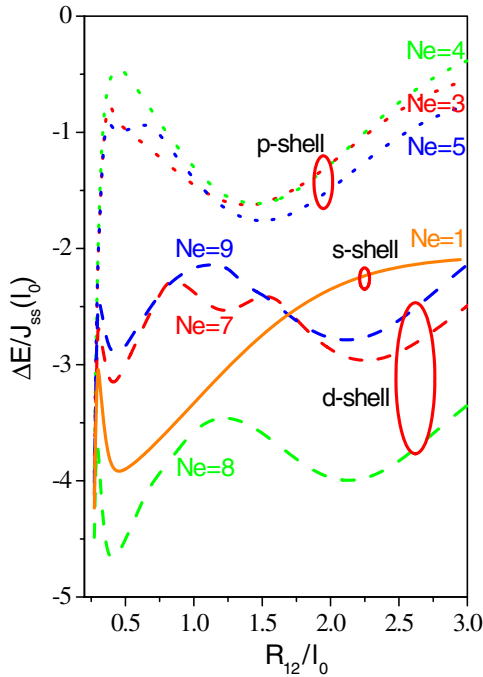


FIG. 3 (color online). Energy shift  $\Delta = E_c - E_e$ , as a function of separation between two Mn ions, one located at the center of the quantum dot and the second one on the  $x$  axis, for different electron numbers  $Ne$ . Results for partially filled  $s$ ,  $p$ , and  $d$  electronic shells are shown.

Hamiltonian, Eq. (3). We find the degenerate ground state of the hybrid system, with electron spin parallel to the total Mn spin, and energy  $E(M, +) = -(J_{ss}/2)M + (J_{12}/2) \times [M(M+1) - \frac{35}{2}]$ . In the absence of coupling to the electron spin ( $J_{ss} = 0$ ), the ground state energy is minimized for the total Mn spin  $M = 0$ , i.e., antiferromagnetic Mn arrangement. However, coupling to the electron spin gives the minimum energy of the hybrid system for finite total Mn spin  $M^* = [(J_{ss}/J_{12}) - 1]/2$ . We can reach different spin alignments, i.e., ferromagnetic ( $M^* = 5$ ), canted ( $0 < M^* < 5$ ), and antiferromagnetic ( $M^* = 0$ ) by adjusting the ratio  $\delta = J_{ss}/J_{12}$  with proper choice of the positions of a pair of Mn ions. For  $M = M^* = [(J_{ss}/J_{12}) - 1]/2$ , the energy is found to be  $E(M^*, +) = -(J_{12}/8)\{[(J_{ss}/J_{12}) - 1]^2 + 70\}$ . It is negative; i.e., the magnetopolaron is formed. The binding energy of the magnetopolaron is a nonmonotonic function of Mn-Mn separation due to two different length scales, the decay  $\lambda$  of short-range antiferromagnetic interaction, and decay  $\ell_0 = 1/\sqrt{\omega_0}$  of ferromagnetic carrier induced interaction. This is illustrated in Fig. 3, where energy shift  $\Delta$  of the ground state energy, the magnetopolaron energy, is shown for the  $Ne = 1$  electron from exact diagonalization of the full Hamiltonian, Eq. (1). The energy is negative and shows nonmonotonic dependence on the length scale where  $J_{12}$  dominates and a smooth decay on the length scale of a quantum dot where  $J_{ss}$  dominates. The formation of magnetopolarons in partially filled  $p$  and  $d$  shells is also shown in Fig. 3. The

magnitude of polaron energy and its dependence on distance is found to depend strongly on the partially filled shell and the degree of filling.

In summary, we formulate a theory of carrier mediated Mn-Mn interactions in quantum dots. The interaction is classified by electron numbers into two regimes: (a) closed shells with RKKY interactions and (b) partially filled shells where nonperturbative magnetopolaron effects dominate. We derive explicit expressions for RKKY interaction and present many-electron magnetopolaron energies for the first three quantum dot shells. This opens up the possibility to engineer magnetic properties on nanoscale using quantum dots containing magnetic ions and an electrically tunable number of carriers.

P. H. acknowledges the support of the Canadian Institute for Advanced Research and the NRC-Helmholtz collaborative grant. F. Q. acknowledges support by UFU-BRAZIL, by the Institute for Microstructural Sciences, NRC Canada, and by NSERC.

- [1] A. Sachrajda, P. Hawrylak, and M. Ciorga, in *Transport in Quantum Dots*, edited by J. Bird (Kluwer, New York, 2003), Chap. 3.
- [2] A. J. Heinrich, J. A. Gupta, C. P. Lutz, and D. M. Eigler, *Science* **306**, 466 (2004).
- [3] J. K. Furdyna, *J. Appl. Phys.* **53**, 7637 (1982).
- [4] P. Hawrylak, M. Grabowski, and J. J. Quinn, *Phys. Rev. B* **44**, 13 082 (1991).
- [5] Jürgen König, Hsiu-Hau Lin, and Allan H. MacDonald, *Phys. Rev. Lett.* **84**, 5628 (2000).
- [6] Mona Berciu and R. N. Bhatt, *Phys. Rev. Lett.* **87**, 107203 (2001).
- [7] A. M. Yakunin *et al.*, *Phys. Rev. Lett.* **92**, 216806 (2004).
- [8] D. M. Hoffman *et al.*, *Solid State Commun.* **114**, 547 (2000).
- [9] A. L. Efros, M. Rosen, and E. I. Rashba, *Phys. Rev. Lett.* **87**, 206601 (2001).
- [10] Steven C. Erwin *et al.*, *Nature (London)* **436**, 91 (2005).
- [11] C. Gould *et al.*, cond-mat/0501597.
- [12] S. Mackowski *et al.*, *Appl. Phys. Lett.* **84**, 3337 (2004).
- [13] L. Besombes, Y. Leger, L. Maingault, D. Ferrand, and H. Mariette, *Phys. Rev. Lett.* **93**, 207403 (2004); **95**, 047403 (2005).
- [14] J. Fernández-Rossier and L. Brey, *Phys. Rev. Lett.* **93**, 117201 (2004).
- [15] Alexander O. Govorov, *Phys. Rev. B* **70**, 035321 (2004); **72**, 075359 (2005).
- [16] Fanyao Qu and Pawel Hawrylak, *Phys. Rev. Lett.* **95**, 217206 (2005).
- [17] M. A. Ruderman and C. Kittel, *Phys. Rev.* **96**, 99 (1954).
- [18] Maxim G. Vavilov and Leonid I. Glazman, *Phys. Rev. Lett.* **94**, 086805 (2005).
- [19] S. Raymond *et al.*, *Phys. Rev. Lett.* **92**, 187402 (2004).
- [20] H. Drexler, D. Leonard, W. Hansen, J. P. Kotthaus, and P. M. Petroff, *Phys. Rev. Lett.* **73**, 2252 (1994).
- [21] Y. Shapira, Jr. and N. F. Olivera, *Phys. Rev. B* **35**, 6888 (1987).